

Hydrology, geochemistry and Sr isotopes in solids and solutes of the meltwater from Mittivakkat Gletscher, SE Greenland*

Birgit Hagedorn^{1,†} and Bent Hasholt²

¹Institute of Geochemistry, University of Göttingen, Germany

[†]Present address: Quaternary Research Center and Department of Earth and Space Sciences, Box 351360, University of Washington, Seattle, WA, 98195, USA. E-mail: hagedorn@u.washington.edu

²Institute of Geography, University of Copenhagen, Øster Voldgade 10, DK 1350 Copenhagen, Denmark.

Received 1 November 2003; accepted in revised form 26 June 2004

Abstract This study was initiated to investigate elemental fractionation and Sr isotope systematics associated with glacial erosion by direct comparison of particulate and dissolved load in glacial runoff. Discharge measurements along with chemical and Sr isotope investigations were carried out at the Mittivakkat Gletscher (Glacier), Ammassalik Ø, Southeast Greenland. Major bedrock types are the Ammassalik Intrusive Complex (AIC) of mafic composition and garnet–granite gneiss (GGG) of acidic composition. Mechanical denudation rates (1 mm a^{-1}) reflected in the major outflow are in the range of temperate valley glaciers in Norway. Chemical denudation rates ($32 \text{ t km}^{-2} \text{ a}^{-1}$) and estimated rates of CO_2 drawdown by silicate weathering ($720\text{--}100 \text{ kg C km}^{-2} \text{ a}^{-1}$) are low compared to global mean and match values measured for High Arctic glaciers on Svalbard. The contrast in chemical and Sr isotope composition of bedrock makes Sr isotope ratios a powerful tool for determining source areas of solid and dissolved load. High Ca/K ratios in water compared to suspended particulate matter (SPM) indicate faster dissolution of Ca minerals. By contrast, in GGG bedrock, where biotite and K-feldspar are abundant, Sr isotope ratios in solutes are higher than in SPM, supporting preferential release of ^{87}Sr from a K-mineral lattice.

Keywords Chemical weathering; CO_2 drawdown; element fractionation; glacial erosion; Sr isotopes

Introduction

Interest in chemical denudation associated with glaciers and glaciations has grown largely because of the hypothesis that tectonic uplift could enhance chemical weathering, thereby reducing atmospheric CO_2 , and causing cooling of the Earth (Raymo and Ruddiman 1992). Following this line of reasoning, production of sediments with increased surface areas caused by glacial grinding may result in increased chemical weathering, causing CO_2 drawdown during glacial erosion. General circulation models suggest that future climatic warming, associated with changing atmospheric composition, will be most intense around the Arctic Circle (Hansen *et al.* 1988). In this context, chemical denudation associated with high-latitude glaciers are of special interest because of the potential feedback on CO_2 sequestration due to glacial retreat.

A study by Anderson *et al.* (1997) indicates, however, that glaciers may not increase total chemical denudation rates, but may yield compositionally distinct chemical fluxes due to disruption of mineral lattices by abrasion. A compilation of chemical denudation rates and atmospheric CO_2 sequestration in glacier basins of Svalbard by Hodson *et al.* (2000) indicates transient CO_2 drawdown rates in the range of $110\text{--}3000 \text{ kg C km}^{-2} \text{ a}^{-1}$, which is within the lower rates estimated for glaciers in the northern hemisphere ($110\text{--}13\,000 \text{ kg C km}^{-2} \text{ a}^{-1}$). Chemical weathering and CO_2 drawdown depends primarily

*Paper presented at the 14th Northern Research Basins Symposium/Workshop (Kangerlussuaq, Søndre Strømfjord, Greenland, 25–29th August 2003).

on specific discharge and secondarily on lithology. Chemical denudation is most active in regions dominated by basaltic and carbonaceous lithologies.

Sr isotope systematic in surface processes

The $^{87}\text{Sr}/^{86}\text{Sr}$ ratio of minerals is unique and therefore provides a useful tracer to determine and quantify sources of solid and dissolved phases in the Earth's surface processes (Capo *et al.* 1998; Stewart *et al.* 1998). The decay of ^{87}Rb to ^{87}Sr with a half-life of 4.2×10^9 years results in a gain in ^{87}Sr over time. Minerals with high Rb and low Sr concentrations have relatively high $^{87}\text{Sr}/^{86}\text{Sr}$ ratios. Since Rb substitutes for K, and Sr substitutes for Ca in mineral lattices, K minerals have higher $^{87}\text{Sr}/^{86}\text{Sr}$ ratios than Ca minerals in the same rock.

There is a strong interest in understanding Sr isotope ratios in glacial runoff in connection with the variation in the Sr isotope composition preserved in marine biogenic carbonates, which are widely regarded as the most detailed proxy of continental Sr fluxes to the ocean. The increase in $^{87}\text{Sr}/^{86}\text{Sr}$ over the last 40 Ma is generally interpreted as an increase in transport of radiogenic Sr (^{87}Sr) to the oceans due to an increase in continental chemical weathering (Palmer and Elderfield 1985). High Sr concentrations and high $^{87}\text{Sr}/^{86}\text{Sr}$ ratios in Himalayan rivers make the Himalayan uplift and the associated increase of chemical weathering an attractive explanation for the increase in radiogenic Sr in ocean sediments. Alternatively, continental glaciations could conceivably be responsible for the increase in marine $^{87}\text{Sr}/^{86}\text{Sr}$ ratios (Armstrong 1971; Hodell *et al.* 1990). Glacial grinding of bedrock creates fresh mineral surfaces that are highly susceptible to chemical weathering. Field studies by Anderson *et al.* (2000) and Blum and Erel (1995, 1997) show that dissolution of K-bearing minerals (mica, K-feldspar) in young glacial deposits causes disproportionate increases in Sr isotope ratios in stream runoff. Recent investigations by Sharp *et al.* (2002) of stream runoff from the Robertson Glacier, Canada indicate that trace amounts of K-bearing minerals (microcline, muscovite) in subglacial basins can increase the Sr isotope composition over those of carbonate bedrock. These studies suggest that an increase in Sr isotope ratios in the marine record may be related to periods of more active glacial erosion instead of increased rates of weathering of silicates and of atmospheric CO_2 drawdown by chemical weathering. However, detailed studies of Sr isotopes systematic in glacial runoff to assess this hypothesis are still underrepresented.

Our paper presents Sr isotope and chemical data along with discharge measurements of suspended and dissolved material eroded by a retreating glacier. Sr isotope ratios have been used to determine source areas of solids and solutes. The direct comparison of isotopic and chemical composition of sediment and solutes provides insights into element and isotope fractionation processes associated with glacial erosion.

The study area

The Mittivakkat Gletscher ($65^\circ 41' \text{N}$, $37^\circ 48' \text{W}$) is the largest single glacier in a snow and ice covered area on the Angmassalik Ø, Southeast Greenland (Figure 1). The mean annual air temperature is -1.6°C and annual precipitation is 983 mm.

At present the glacier covers an area of 17.6 km^2 and the average ice thickness is 115 m (Knudsen and Hasholt 1999). The major bedrock underlying the glacier is the Ammassalik Intrusive Complex (AIC) intruded 1.9 Ga ago (Hansen and Kalsbeek 1989). Garnet-granite gneiss (GGG) envelops the AIC (Friend and Nutman 1989) at the western and northern border and foreland of the glacier. Sr isotope ratios range between 0.70419 and 0.70939 for AIC-bedrock and between 0.7089 and 0.7247 for GGG-bedrock (Kalsbeek *et al.* 1993). Both bedrock types contain biotite, while K-feldspar occurs in GGG-bedrock only. Since both K-minerals increase Sr isotope ratios, the higher $^{87}\text{Sr}/^{86}\text{Sr}$ for GGG-bedrock may be attributed to K-feldspar. Changes in the extent of the glacier since 1933 are well documented (Frstrup

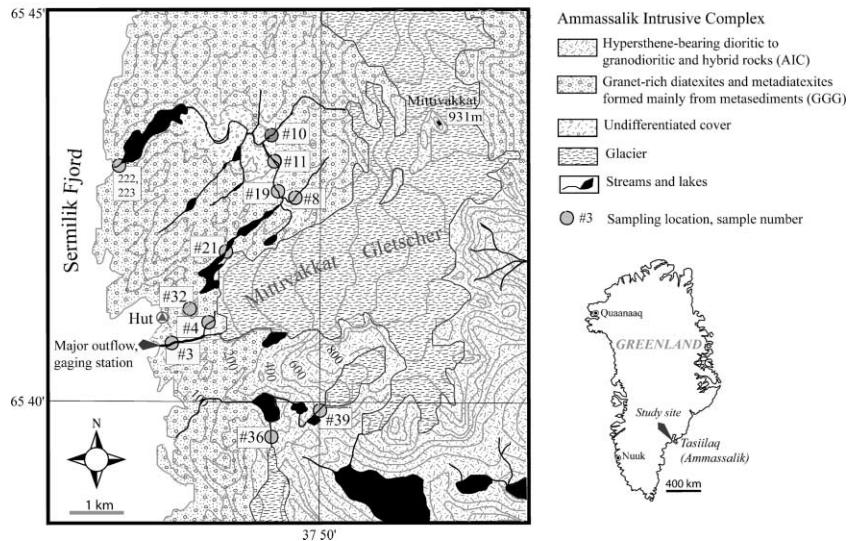


Figure 1 Geological map of the Mittivakkat area with sampling locations. Source: Geological Survey of Denmark and Greenland, compiled by C. Escher

1960; Hasholt 1986, 1992; Valeur 1959) and data indicate an almost continuous retreat that is most pronounced along the western and northern margins. The mean surface lowering of about 5.8 m indicates a mean net balance of 0.43 m water per year. Radio-echo sounding at the Mittivakkat Gletscher indicates marked relief underneath the glacier with two major subglacial depressions that likely have a strong influence on subglacial drainage (Knudsen and Hasholt 1999). The major outflow (location no. 3 in Figure 1) is in the southwest end of the glacier with an annual discharge of approximately $30 \times 10^6 \text{ m}^3 \text{ a}^{-1}$ and suspended sediment load of more than $220 \text{ t km}^{-2} \text{ a}^{-1}$. Another outflow, located in the northwest, drains into a proglacial lake and runs through a string of lakes to the coast 5 km north of the main outlet. A minor proglacial lake is located along the south boundary of the glacier. Glaciers sharing the divide with the Mittivakkat glacier drain to basins south of the area.

Methods

Discharge measurements, water and sediment sampling and procedures for chemical analyses are described in Hasholt and Hagedorn (2000). For Sr separation, samples were dissolved in 2.5N HCl after digestion/evaporation. Sr was separated with standard methods using ion exchange columns with AG50x8 resin 200–400 mesh. Sr isotopes were measured using the rhenium double filament technique (Dickin 1995) on a MAT 262 RPQ⁺® Thermion mass spectrometer. The external accuracy for Sr isotope ratios was checked with the NBS standard 987 as 0.710245 ± 0.000012 ($N = 40$). Sr blanks for sample preparation are below 500 pg. Strontium isotope ratios were normalized to a common $^{86}\text{Sr}/^{88}\text{Sr}$ ratio of 0.1194.

Results and discussion

Suspended matter (SPM) and stream water were collected from different outflows of the Mittivakkat Gletscher, from two local glaciers further south that cover AIC bedrock only, as well as from small streams fed by snow patches. Figure 1 gives an overview of the geology of the area and of the sampling location. Due to very low SPM concentration in the meltwater of snow patches, only its chemistry was analyzed.

Discharge pattern and denudation rate

Discharge was measured at the main outlet near the coast (Figure 1), where a stage was recorded every 10 minutes from June to September. Daily values vary between 2 and $4 \text{ m}^{-3} \text{ s}^{-1}$ and SPM concentration varies between $300\text{--}1500 \text{ mg l}^{-1}$. Tributaries in the north and smaller glaciers in the south were sampled and measured during a 2-week field period from 5–14 August 2000.

Table 1 gives a summary of specific runoff, SPM content, electrical conductivity and drainage area for the different outflows of the Mittivakkat Gletscher. The measurements were performed during a typical rainy period that is representative for this time of the year. During the time of observation, the major outflow of the Mittivakkat Gletscher transported about 10–100 times more sediment, 2–12 times more water, but only 1–3 times more solutes per area than outlets in the north. Sediment content along the water course from the northern proglacial lake (no. 21) to the outflow into Sermilik Fjord (223, 222) decreases by about 65%, indicating sedimentation processes along the water course.

Solute concentrations are rather uniform in the observed streams. The total solute transport from northern outflows and tributaries into the Sermilik Fjord is 2.7 t d^{-1} and exceeds 3 times the suspended sediment flux (0.95 t d^{-1}). In comparison, the suspended sediment flux in the major outflow stream is about 17 times higher than the solute flux. Taking the measured values as the mean daily average and assuming 120 days of discharge would yield an annual mechanical denudation rate of $\sim 0.4 \text{ mm a}^{-1}$ for the entire drainage area and 1 mm a^{-1} (using $220 \text{ t km}^{-2} \text{ a}^{-1}$ for the glacier) for the Mittivakkat Gletscher itself. Such a denudation rate is typical of polar and thin temperate plateau glaciers and of temperate valley glaciers on crystalline bedrock in Norway (Hallet *et al.* 1996). It slightly exceeds sediment denudation rates observed from a cold-based glacier in Svalbard (Hodson *et al.* 1998). However, the present measurements neglect bed load transport and therefore provide minimum denudation rates only. The calculated total solute yields are $11 \text{ t km}^{-2} \text{ a}^{-1}$ for the entire area and $32 \text{ t km}^{-2} \text{ a}^{-1}$ for the major outflow. These values are comparable to glaciers on crystalline bedrock in Svalbard (Hodson *et al.* 2000).

Sr isotope and element composition

Suspended particulate matter. The chemistry and Sr isotope ratios of SPM are summarized in Table 2. The SPM from different outflows and bedrock areas can clearly be differentiated by chemical and Sr isotope composition. The most striking features are high Ca/K ratios of SPM from local glaciers that cover AIC bedrock and major outflow of the Mittivakkat Gletscher relative to those from the northern outflows that drain GGG bedrock only. The higher K concentrations in SPM from GGG bedrock are consistent with observed high abundances of biotite and K-feldspar in this bedrock, while AIC bedrock has a lower biotite content and no K-feldspar.

The Sr isotope ratios and concentrations are displayed in Figure 2 together with bedrock data published by Kalsbeek *et al.* (1993). The collected SPM can be divided into 2 groups. The major outflow and local glaciers have low $^{87}\text{Sr}/^{86}\text{Sr}$ ratios (0.7069–0.7079) and high Sr concentrations, and are close to the Sr isotope ratios of AIC bedrock. The northern outflows have higher $^{87}\text{Sr}/^{86}\text{Sr}$ ratios (0.7149–0.7145) and lower Sr concentrations, and are close to the Sr isotope ratios of GGG bedrock (Kalsbeek *et al.* 1993). The high $^{87}\text{Sr}/^{86}\text{Sr}$ ratios found in northern outflows (nos. 21 and 11) suggest only a minor contribution from the major subglacial basin to SPM, while the low $^{87}\text{Sr}/^{86}\text{Sr}$ ratios in the major outflow indicate that SPM is mainly generated within the subglacial drainage basin. The low Sr concentrations of all SPM compared to bedrock (Figure 2) may reflect weathering and release of mobile alkaline earth elements to water during sediment weathering.

Table 1 Summary of discharge (Q), suspended sediment (SPM) and solute concentrations in the investigated streams of the Mittivakkat Gletscher. Solute concentration is calculated by $0.725EC = \text{mg l}^{-1}$

| Location | Sample no. | Date | Area km ² | Glacier cover % | EC μScm^{-1} | SPM mgL ⁻¹ | Q t km ⁻² d ⁻¹ | SPM kg km ⁻² d ⁻¹ | Solutes kg km ⁻² d ⁻¹ |
|-----------------|-------------|---------|-------------------------|--------------------|----------------------------|--------------------------|---|--|--|
| Major outflow | average | 8/5/00 | 18.30 | 77 | 22.8 | 290.4 | 17941 | 5245 | 273 |
| | min | 8/5/00 | | | | 266.0 | 16525 | 4396 | |
| | max | 8/5/00 | | | | 314.8 | 19357 | 6094 | |
| N. icefall lake | no. 21, 253 | 8/7/00 | 6.08 | 54 | 22.7 | 33.0 | 10757 | 355 | 177 |
| | 174 | 8/6/00 | | | | 26.5 | 264 | | |
| | 254 | 8/6/00 | | | | 31.4 | 312 | | |
| | 255 | 8/6/00 | | | | 24.5 | 244 | | |
| E. tributary | no. 8, 257 | 8/6/00 | 3.81 | 38 | 17.1 | 9.6 | 6803 | 65 | 84 |
| | 261 | 8/7/00 | | | | 11.6 | 126 | 132 | |
| Confluence | no. 19, 260 | 8/7/00 | 9.38 | 35 | 19.5 | 9.2 | 11394 | 105 | 161 |
| | 173 | 8/7/00 | | | | 18.8 | 201 | | |
| | no. 11, 258 | 8/6/00 | | | | 10.00 | 47 | 21.3 | 5.9 |
| N. tributary | no. 10, 259 | 8/6/00 | 5.20 | 13 | 20.4 | 11.8 | 5599 | 66 | 83 |
| Coast | 222 | 8/19/00 | 28.70 | 19 | 24.7 | 6.3 | 5268 | 33 | 94 |
| | 223 | 8/19/00 | | | | 8.7 | 46 | | |

Table 2 Chemistry and Sr isotope ratios of suspended matter (SPM)

| Sample | $^{87}\text{Sr}/^{86}\text{Sr}$ | Sr mg kg^{-1} | CaO wt % | K ₂ O wt % |
|--------|---------------------------------|---------------------------|-------------|--------------------------|
| No. 3 | 0.706899 | 539 | 3.33 | 1.44 |
| No. 21 | 0.714897 | 223 | 1.43 | 1.55 |
| No. 11 | 0.714931 | 141 | 0.85 | 0.93 |
| No. 19 | 0.714520 | 220 | 0.92 | 0.96 |
| No. 39 | 0.707911 | 413 | 1.96 | 0.98 |
| No. 36 | 0.707627 | 547 | 2.28 | 1.11 |

Stream water. All observed stream waters have electrical conductivities between 16 and $30 \mu\text{S cm}^{-1}$, and pH values around 6.5. The rates at which elements are derived from the bedrock through rock weathering and atmospheric CO_2 is consumed by silicate weathering were calculated following the procedure described in Sharp (1995) using element concentrations measured in stream water and element/Cl ratios measured in glacial ice and snow pack ($n = 38$) (Table 3). The chemical composition expressed as % element content from the total element concentration is displayed in Figure 3. Here the element concentrations are corrected for precipitation using element/Cl ratios of glacial water. The dominant cation in all water is Ca^{2+} . Water draining GGG bedrock is characterized by high K/Ca ratios and SO_4^{2-} concentration, indicating a higher contribution by pyrite oxidation and weathering of K-bearing minerals than in water draining AIC bedrock. The high SO_4^{2-} and relatively low HCO_3^- concentration suggest that oxidation of sulfides is the major source of protons for silicate hydrolysis. In contrast, water draining AIC bedrock is rich in HCO_3^- , which balances silicate hydrolysis and carbonation reaction and may even reflect trace quantities of calcite in the rocks.

Maximum values of CO_2 drawdown by silicate weathering are estimated to be between 720 (major outflow) and $100 \text{ kgC km}^{-2} \text{ a}^{-1}$. These values are comparable to values observed for Svalbard glaciers, the Erdmansbreen and Midtre Lorenbreen (Hodson *et al.* 2000), but are much lower than global mean values ($3000 \text{ kgC km}^{-2} \text{ a}^{-1}$) estimated by Gaillardet *et al.* (1999) and values estimated from other glacier-covered areas (e.g. Alaska or Iceland, summarized in Hodson *et al.* (2000)).

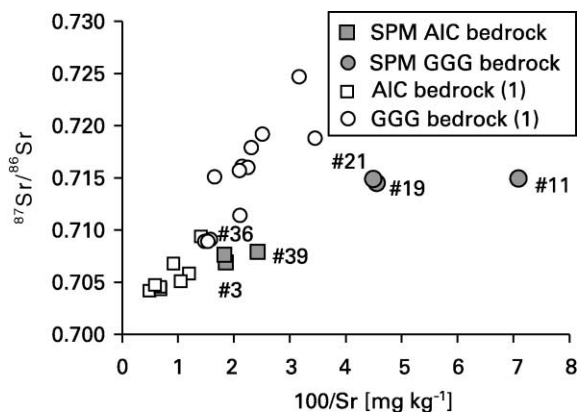


Figure 2 $^{87}\text{Sr}/^{86}\text{Sr}$ ratios versus $100/\text{Sr}$ of SPM indicate high $^{87}\text{Sr}/^{86}\text{Sr}$ ratios for SPM from the major outflow and local small glaciers, consistent with AIC bedrock. SPM from northern outflows have high $^{87}\text{Sr}/^{86}\text{Sr}$ ratios consistent with GGG bedrock. Low Sr concentrations in SPM relative to bedrock probably reflect chemical weathering of sediment. Values for bedrock are from Kalsbeek *et al.* (1993)

Table 3 Chemistry and Sr isotope ratios of stream water. n.d. = not detected

| Sample no. | Ca ²⁺ mg L ⁻¹ | K ⁺ mg L ⁻¹ | Mg ²⁺ mg L ⁻¹ | Na ⁺ mg L ⁻¹ | Si _(aq) mg L ⁻¹ | Cl ⁻ mg L ⁻¹ | SO ₄ ⁻² mg L ⁻¹ | HCO ₃ ⁻ mg L ⁻¹ | Sr ²⁺ μg L ⁻¹ | ⁸⁷ Sr/ ⁸⁶ Sr |
|--------------------|--|--------------------------------------|--|---------------------------------------|--|---------------------------------------|---|---|--|------------------------------------|
| No. 3 | 1.18 | 0.30 | 0.50 | 1.27 | 0.33 | 2.28 | 2.7 | 2.52 | 12 | 0.712831 |
| No. 21 | 1.26 | 0.30 | 0.60 | 1.26 | 0.44 | 2.58 | 3.89 | 1.23 | 9.7 | 0.717618 |
| No. 11 | 1.10 | 0.27 | 0.49 | 1.18 | 0.58 | 2.00 | 4.17 | 0.56 | 13 | 0.711824 |
| No. 19 | 1.02 | 0.25 | 0.45 | 1.07 | 0.50 | 1.87 | 3.83 | 0.47 | 12 | 0.711772 |
| No. 8 | 1.25 | 0.57 | 0.42 | 1.66 | 0.67 | n.d. | n.d. | n.d. | 18 | n.d. |
| No. 10 | 1.08 | 0.27 | 0.33 | 1.35 | 0.59 | 1.94 | 3.76 | 0.79 | 10 | 0.717789 |
| No. 39 | 0.96 | 0.10 | 0.42 | 0.87 | 0.37 | 1.42 | 1.01 | 3.73 | 37 | 0.708543 |
| No. 36 | 1.21 | 0.10 | 0.46 | 0.90 | 0.30 | 1.94 | 2.64 | 1.81 | 20 | 0.706927 |
| No. 4 | 1.22 | 0.22 | 0.52 | 0.32 | 0.36 | 0.86 | 4.93 | 0 | 7.5 | 0.712435 |
| No. 32 | 1.66 | 0.26 | 0.64 | 3.00 | 1.08 | 4.90 | 2.52 | 4.88 | 10 | 0.720195 |
| Snow <i>n</i> = 21 | 0.05 | 0.06 | 0.10 | 1.04 | n.d. | 1.82 | 0.28 | n.d. | n.d. | n.d. |
| Stdev | 0.04 | 0.05 | 0.13 | 1.00 | n.d. | 1.93 | 0.29 | n.d. | n.d. | n.d. |

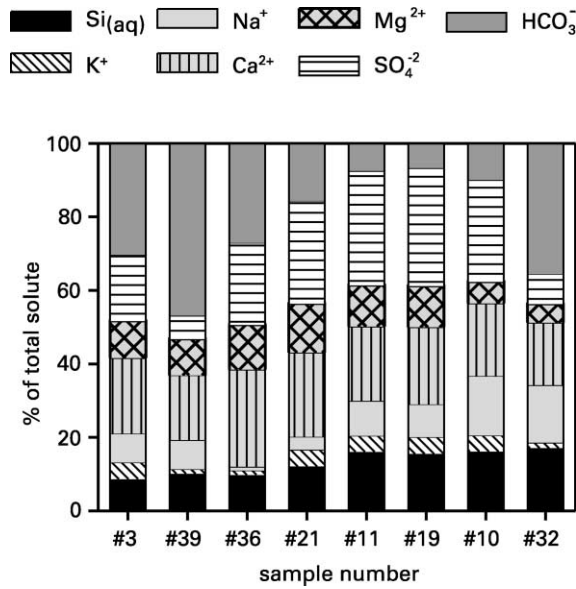


Figure 3 Elemental composition of water expressed as % of total solute concentration ($\mu\text{mol l}^{-1}$). Samples from northern outflows have higher SO_4^{-2} and K^+ concentrations than water from small local glaciers

The Sr isotope compositions of stream water in the different outflows are quite distinct from one another (Figure 4). Streams fed by local glaciers in the south have low isotope ratios (0.7069–0.7085) and high Sr concentrations. The outflow of the proglacial lake (no. 21) north of the Mittivakkat Gletscher and the outflow in the far northeast (no. 10) have higher Sr isotope ratios (0.716–0.718) and relatively low Sr concentrations. The high Sr isotope ratio measured in meltwater (no. 32) of a snow patch in GGG bedrock further suggests that GGG bedrock is a viable source of high Sr isotope ratios. The major outflow of the Mittivakkat Gletscher to the west (no. 3) as well as the confluence (nos. 19 and 11) of the

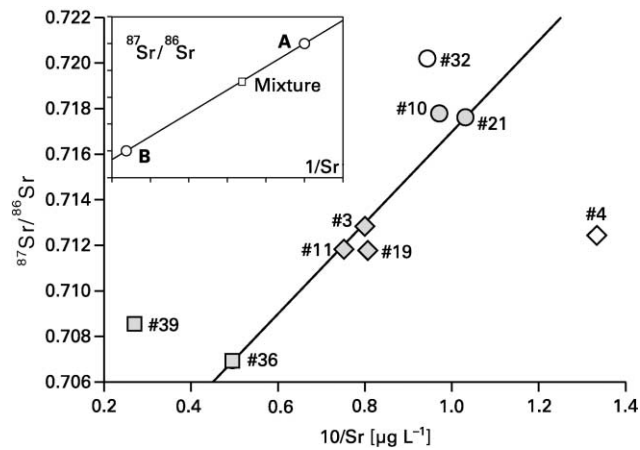


Figure 4 Sr isotope compositions versus inverse Sr concentration of water samples. Water from northern outflows has a higher $^{87}\text{Sr}/^{86}\text{Sr}$ than water from local small glaciers. The positive regression line can be regarded as a mixing line (see insert), indicating that samples nos. 3, 11 and 19 are a mixture of water draining AIC bedrock only (no. 36) and water draining GGG bedrock only (no. 21). (Open symbols are samples from melting snow patches, diamonds indicate a mixture of AIC and GGG bedrock)

outflow of the proglacial lake (no. 21) and eastern tributary (no. 8) have Sr isotope ratios between the proglacial lake and local glaciers, and lie on a regression line between the local glacier in the south (no. 36) and northern outflow (no. 21). Presuming that the solute denudation rate is equal within each glacial sub-basin and between the local and major glacier, the regression line can be regarded as a mixing line, allowing the calculation of contribution of each bedrock type to the outflows by Equation (1) (Albarède 1996):

$$R_M = R_A(f_A C_A / C_M) + R_B^*(f_B C_B / C_M) \quad (1)$$

where R is $^{87}\text{Sr}/^{86}\text{Sr}$, C is the Sr concentration of end members A , B and mixture M , f is the fraction of phase A and B in M ; ($f_B = 1 - f_A$).

Using samples from the local glacier in the south (no. 36) and from the proglacial lake (no. 21) as end-members for AIC (A) and GGG (B) bedrock, respectively, in Equation (1), approximately 70% of Sr in the major outflow is derived from weathering of GGG bedrock. The isotope ratios measured in sample no. 4, collected from a stream fed by a snow patch below the western border of the glacier, are identical with the major outflow. This suggests that sediments deposited in front of the glacier mouth are most likely the Sr source of the major outflow. The lower Sr concentration of sample no. 4 compared to sample no. 3 can be attributed to higher dilution by meltwater with low Sr concentrations.

The $^{87}\text{Sr}/^{86}\text{Sr}$ ratio for the eastern tributary (no. 8) of the confluence has not been measured but can be calculated by means of the measured Sr concentration ($18.5 \mu\text{g l}^{-1}$) and calculated regression line shown in Figure 4 (Faure 1986):

$$R_M = R_i + 1/C_M^* m \quad (2)$$

where R is $^{87}\text{Sr}/^{86}\text{Sr}$, C is the Sr concentration ($\mu\text{g l}^{-1}$) M is the mixture, m is the slope of the regression line, while subscript M indicates mixture and i the y-intercept.

This calculation yields an isotope ratio of 0.70725 for no. 8 and suggests that AIC bedrock is the dominant Sr source. Using this isotope ratio in Equation (1) indicates that the outflow of the proglacial lake contributes approximately 60% and the eastern tributary about 40% to the confluence. Recalculating the discharge for the eastern tributary yields $0.50 \text{ m}^3 \text{ s}^{-1}$ and is in good agreement with the measured value of $0.48 \text{ m}^3 \text{ s}^{-1}$ (Table 1).

Comparison of solid and dissolved load

Significant isotopic differences between SPM and dissolved load are observed for almost all water samples. Assuming that SPM reflects the average chemical and isotope composition of bedrock that reacts with water, the observed isotope disequilibrium between the solid and dissolved phase can be attributed to at least four processes operating individually or collectively: (1) fast release of ^{87}Sr from a biotite lattice leading to higher Sr isotope ratios in solutes; (2) fast release of Ca (and therefore Sr) due to dissolution of Ca-rich minerals (Lasaga *et al.* 1994), which may be accelerated by glacial grinding (Anderson *et al.* 2000; Sharp *et al.* 2002) leading to lower Sr isotope ratios in solutes; (3) mobilization (activation) of different source areas of suspended and dissolved load; and (4) fractionation of sediments from solutes due to sedimentation along the watercourse.

All waters have higher Ca/K ratios than SPM, indicating preferential weathering of Ca-rich minerals. SPM and the dissolved load from samples of local glaciers are closest in isotope equilibrium, whereas sample no. 36 has lower isotope ratios and sample no. 39 has higher isotope ratios in water than in SPM. Together with an increase in Ca/K ratio by a factor of 10 the lower isotope ratio in sample no. 36 indicates fast dissolution of Ca silicates and/or carbonate. The slightly higher Sr isotope ratio of no. 39, however, may indicate a contribution of K-bearing minerals that is supported further by the lower Ca/K ratio compared to sample no. 36. Since K-feldspar does not occur in AIC bedrock, the higher

Sr isotope ratios are most likely due to biotite weathering. An increase in $^{87}\text{Sr}/^{86}\text{Sr}$ through K-feldspar and muscovite dissolution in delayed flow water, where reaction time with rocks is high, has been observed by Sharp *et al.* (2002) in Canadian glaciers. The high Sr isotope ratios observed in northern outflows that drain GGG bedrock exclusively are best explained by biotite and K-feldspar weathering that are abundant in GGG bedrock. The higher contribution of K-bearing minerals to the dissolved load is also indicated by the weaker enrichment of Ca relative to K in water from the northern outflows compared to local glaciers. The Sr isotope signature of AIC bedrock in the SPM indicates AIC bedrock as a major source for SPM in the major outflow of the Mittivakkat Gletscher and local glaciers (Figure 2). In contrast, the Sr isotope signature of solutes indicates that approximately 70% of the Sr in the major outflow is from weathering of GGG bedrock. The good agreement between Sr isotope ratios of the major outflow with snowmelt water in front of the glacier mouth suggest that the weathering of recent glacial deposits in front of the glacier mouth, which are a mixture of GGG and AIC bedrock, may increase the Sr isotope ratio of the major outflow after it emerged from the subglacial basin. These observations are consistent with studies by Anderson *et al.* (1997), Blum and Erel (1997) and Clow *et al.* (1997) in young biotite-containing glacial deposits.

The lower Sr isotope ratios in water compared to SPM found in samples nos. 11 and 19 after the confluence of the proglacial lake and eastern tributary can most likely be explained by post-glacial mixing processes in connection with sediment re-deposition in the streams. The decrease in $^{87}\text{Sr}/^{86}\text{Sr}$ ratios in water after the confluence is in agreement with the low Sr isotope ratio of sample no. 8, as derived from mixing calculations. In contrast, the Sr isotope ratio of SPM after the confluence remains high, indicating that the majority of SPM is most likely from the outflow of the proglacial lake. A possible explanation could be the preferential settling of SPM transported by eastern tributaries after its confluence with the proglacial lake. Such sediment settling processes are supported by the low SPM concentration (9.2 mg l^{-1}) at the confluence, compared to calculated SPM concentrations from discharge measurements of both tributaries (24 mg l^{-1}). However, this suggestion cannot be verified, since we did not measure the isotope signature of the eastern tributary.

Summary and conclusions

Suspended sediment and water samples were collected and discharge was measured during a 2-week field survey in 2000. The extension of measurements over such a short period to annual denudation rates should be regarded with caution. However, if the measurements are representative of annual means, calculated rates of mechanical and chemical denudation as well as rates of CO_2 drawdown are low compared to the global mean and other northern glacial areas, but values are comparable to High Arctic glaciers on Svalbard. These modest rates highlight that caution is required when associating glacier activity with rapid erosion and weathering rates. Such associations are clearly justified for large, fast-moving temperate glaciers (Hallet *et al.* 1996), but they are not appropriate for small, slow-moving high-latitude glaciers. In the limit of vanishing basal motion, which is expected for cold-based glaciers, the ice cover would effectively shield the bedrock from erosion and weathering.

Sr isotopes constitute a powerful tool for determining source areas of SPM and solutes. Higher Ca/K ratios measured in water rather than in SPM indicate preferential dissolution of Ca minerals that usually have low Sr isotope ratios. However, with the exception of sample no. 36 all streams have higher $^{87}\text{Sr}/^{86}\text{Sr}$ ratios in water than in SPM, indicating preferential release of ^{87}Sr to water. This effect seems less pronounced in AIC bedrock where only biotite is abundant rather than in GGG bedrock where biotite and K-feldspar are abundant and suggests that not only biotite but also K-feldspar preferentially releases ^{87}Sr during subglacial dissolution.

Acknowledgements

Both authors have contributed equally to the manuscript. We thank Bernard Hallet for discussion and valuable comments on the manuscript, and B. Elberling and O. Seather for reviewing and providing improvements to the text. The project was sponsored by SNF (Statens naturvidenskabelige forskningsråd).

References

- Albarède, F. (1996). *Introduction to Geochemical Modeling*. Cambridge University Press, Cambridge.
- Anderson, P.S., Drever, J.I. and Humphrey, N.F. (1997). Chemical weathering in glacial environments. *Geology*, **25**, 399–402.
- Anderson, S.P., Drever, J.I., Frost, C.D. and Holden, P. (2000). Chemical weathering in the foreland of a retreating glacier. *Geochim. Cosmochim. Acta.*, **64**(7), 1173–1189.
- Armstrong, R.L. (1971). Glacial erosion and the variable isotopic composition of strontium in sea water. *Nature*, **230**, 132–133.
- Blum, J.D. and Erel, Y. (1995). A silicate weathering mechanism linking increases in marine $^{87}\text{Sr}/^{86}\text{Sr}$ with global glaciation. *Nature*, **373**, 415–418.
- Blum, J.D. and Erel, Y. (1997). Rb-Sr isotope systematics of a granitic soil chronosequences: the importance of biotite weathering. *GCA*, **61**, 3193–3204.
- Capo, R.C., Steward, B.W. and Chadwick, O.A. (1998). Strontium isotopes as tracers of ecosystem processes: theory and methods. *Geoderma*, **82**, 197–225.
- Clow, D.W., Mast, M.A., Bullen, T.D. and Turk, J.T. (1997). $^{87}\text{Sr}/^{86}\text{Sr}$ as a tracer of mineral weathering reactions and calcium sources in an alpine/subalpine watershed, Loch Vale, Colorado. *Wat. Res. Res.*, **33**(6), 1335–1351.
- Dickin, A.D. (1995). *Radiogenic Isotope Geology*. Cambridge University Press, Cambridge.
- Faure, G. (1986). *Principles of Isotope Geology*. John Wiley & Sons, New York.
- Friend, C.R.L. and Nutman, A.P. (1989). The geology and structural setting of the Ammassalik Intrusive Complex, South-East Greenland. *Grøn. Geol. Unders.*, **146**, 41–46.
- Fristrup, B. (1960). Studies of four glaciers in Greenland. *Geogr. Tids.*, **69**, 192–204.
- Gaillardet, J., Dupré, B. and Allègre, C.J. (1999). Geochemistry of large river suspended sediments: silicate weathering or recycling tracer? *Geochim. Cosmochim. Acta.*, **63**(23/24), 4037–4051.
- Hallet, B., Hunter, L. and Bogen, J. (1996). Rates of erosion and sediment evacuation by glaciers: a review of field data and their implication. *Glob. Planet. Change*, **12**, 213–235.
- Hansen, B.T. and Kalsbeek, F. (1989). Precise age for the Ammassalik Intrusive Complex. *Grøn. Geol. Unders.*, **146**, 46–47.
- Hansen, J., Fung, I., Laci, A., Rind, D., Lebedeff, S., Ruedy, R. and Russel, G. (1988). Global climate changes as forecast by Goddard Institute of Space Studies three-dimensional model. *J. Geophys. Res.*, **93**, 9341–9364.
- Hasholt, B. (1986). Mapping of the Mitdluagkat Glacier – a preliminary report. *Geogr. Tids.*, **87**, 19–21.
- Hasholt, B. (1992). Sediment transport in a Proglacial Valley. *Geogr. Tids.*, **92**, 105–110.
- Hasholt, B. and Hagedorn, B. (2000). Hydrology and geochemistry of river-born material in a High Arctic drainage system, Zackenberg, Northeast Greenland. *Arct. Antarct. Alp. Res.*, **32**(1), 84–94.
- Hodell, D.A., Mead, G.A. and Mueller, P.A. (1990). Variation in the strontium isotopic composition of seawater (8ma to present): implications for chemical weathering rates and dissolved fluxes to the oceans. *Chem. Geol.*, **80**, 291–307.
- Hodson, A., Gurnell, A., Tranter, M., Bogen, J., Hagen, O.O. and Clark, M. (1998). Suspended sediment yield and transfer processes in a small high-Arctic glacier basin, Svalbard. *Hydrol. Proc.*, **12**, 73–86.
- Hodson, A., Tranter, M. and Vatne, G. (2000). Contemporary rates of chemical denudation and atmospheric CO₂ sequestration in glacier basins: an Arctic perspective. *Earth Surf. Proc. Landf.*, **25**, 1447–1471.
- Kalsbeek, F., Austrheim, H., Bridgewater, D., Hansen, B.T., Pedersen, S. and Taylor, P.N. (1993). Geochronology of Archean and Proterozoic events in the Ammassalik area, South-East Greenland, an comparisons with the Lewisian of Scotland and the Nagssugtiqidian of West Greenland. *Precam. Res.*, **62**, 239–270.
- Knudsen, N.T. and Hasholt, B. (1999). Radio-echo sounding at the Mittivakkat Gletscher, Southeast Greenland. *Arct. Antarct. Alp. Res.*, **31**(3), 321–328.
- Lasaga, A.C., Soler, J.M., Ganor, J., Burch, T.E. and Nagy, K.L. (1994). Chemical weathering rate laws and global geochemical cycles. *Geochim. Cosmochim. Acta.* **58**(10), 2361–2386.

- Palmer, M.R. and Elderfield, H. (1985). Sr isotope composition of sea water over the past 75 Myr. *Nature*, **314**, 526–528.
- Raymo, M.E. and Ruddiman, W.F. (1992). Tectonic forcing of late Cenozoic climate. *Nature*, **359**, 117–122.
- Sharp, M. (1995). Rates of chemical denudation and CO₂ drawdown in glacier-covered alpine catchment. *Geology*, **23**, 61–64.
- Sharp, M., Creaser, P.A. and Skidmore, M. (2002). Strontium isotope composition of runoff from a glaciated carbonate terrain. *Geochim. Cosmochim. Acta.*, **66**(4), 595–614.
- Stewart, B.W., Capo, R.C. and Chadwick, O.A. (1998). Quantitative strontium isotope models for weathering, pedogenesis and biogeochemical cycling. *Geoderma*, **82**, 173–195.
- Valeur, H. (1959). Runoff studies from the Midtluagkat Gletscher in SE-Greenland during late summer 1958. *Geogr. Tids.*, **58**, 209–219.